IMPROVED COMPUTATIONAL TREATMENT OF TRANSONIC FLOW ABOUT SWEPT WINGS

W. F. Ballhaus*, F. R. Bailey†, and J. Frick‡
NASA Ames Research Center

INTRODUCTION

Transonic small-disturbance theory is attractive in practical engineering design and analysis primarily because of the flexibility it offers in the treatment of boundary conditions. The theory can provide an understanding of the physics of complex, three-dimensional transonic flows, without the need of complicating features such as airfoil surface-oriented coordinate transformations, which are generally used in less approximate theories. However, as with any other asymptotic theory, problems can arise when the theory is applied to cases that differ from the assumptions under which it is derived.

Relaxation solutions to classical three-dimensional small-disturbance (CSD) theory for transonic flow about lifting swept wings were first reported in references 1 and 2. A deficiency in the treatment of wings with moderate-to-large sweep angles soon became apparent. For such wings, the CSD theory was found to be a poor approximation to the full potential equation in regions of the flow field that are essentially two-dimensional in a plane normal to the sweep direction. This was pointed out in reference 3, which emphasized determination of the effect of this deficiency on the capture of embedded shock waves in terms of (1) the conditions under which shock waves can exist and (2) the relations they must satisfy when they do exist. A modified small-disturbance (MSD) equation, derived by retaining two previously neglected terms, was proposed and shown to be a consistent approximation to the full potential equation over a wider range of sweep angles. The purpose of this paper is to demonstrate the important effect of these extra terms by comparing CSD, MSD, and experimental wing surface pressures.

THE EXISTENCE OF SHOCK WAVES ON AN INFINITE ASPECT RATIO SWEPT WING

Consider an infinite aspect ratio wing with sweep angle λ. For a vertical shock wave to exist, the flow must be supercritical in a direction normal to the sweep. Since the derivatives of all flow quantities with respect to the span direction are zero, it can be shown that $\phi_y + \phi_x \tan \lambda = 0$, where

---

*Research Scientist, Computational Fluid Dynamics Branch, and U.S. Army AMRDL.

†Research Scientist, Computational Fluid Dynamics Branch.

‡Programmer/Analyst, Informatics, Inc., Palo Alto, Calif.

ϕ_y and ϕ_x are perturbation velocities parallel to the wing plane in the free-stream-normal and free-stream directions, respectively. The condition from the full potential formulation for sonic flow normal to the sweep direction is

$$\phi_x^*(\lambda) = -\cos^2 \lambda \left[1 - \sqrt{1 - \frac{2}{\gamma + 1}\left(1 - (M_\infty^2 \cos^2 \lambda)^{-1}\right)}\right] \tag{1}$$

where the velocity in the free-stream direction is given by $U_\infty(1 + \phi_x)$, and the asterisk denotes critical (sonic) conditions in a direction normal to the shock. A shock with sweep λ can exist whenever $\phi_x^*(\lambda) < \phi_x < (\phi_x)_{MAX}$, where $(\phi_x)_{MAX}$ corresponds to zero sound speed.

For classical small-disturbance theory, the governing equation written in conservation form is

$$\left[(1 - M_\infty^2)\,\phi_x - \frac{(\gamma + 1)}{2} M_\infty^n\, \phi_x^2\right]_x + (\phi_y)_y + (\phi_z)_z = 0 \tag{2}$$

and the equivalent expression for (1) is

$$\phi_x^*(\lambda) = \frac{\sec^2 \lambda - M_\infty^2}{(\gamma + 1)\, M_\infty^n} \tag{3}$$

The exponent n will be specified subsequently. Equations (1) and (3) are compared in figure 1. Note the increasing disparity as the sweep increases. At other than small sweep angles, the CSD equation does not permit the existence of shocks for values of ϕ_x for which they can exist according to the full potential equation.

This situation can be improved by the use of the MSD equation (ref. 3), written here in conservation form

$$\left[(1 - M_\infty^2)\phi_x - \left(\frac{\gamma + 1}{2}\right) M_\infty^n\, \phi_x^2 + \frac{1}{2}(\gamma - 3) M_\infty^p\, \phi_y^2\right]_x + \left[\phi_y - (\gamma - 1) M_\infty^p\, \phi_x \phi_y\right]_y + (\phi_z)_z = 0 \tag{4}$$

The corresponding sonic condition, also plotted in figure 1, is

$$\phi_x^*(\lambda) = \frac{\sec^2 \lambda - M_\infty^2}{(\gamma + 1) M_\infty^n + (\gamma + 1) M_\infty^p \tan^2 \lambda} \tag{5}$$

The MSD equation satisfies two-dimensional sweep theory; i.e., it is as consistent with the full potential equation as the two-dimensional transonic small disturbance theory taken in a plane normal to the sweep. The approximation improves as $M_n = M_\infty \cos \lambda$ approaches unity.

Values of n,p in equation (4) can be selected to improve the approximation for values of M_n that are not close to unity. For example, n,p, can be determined, *for a given* M_∞, to better approximate either the full potential $\phi_x^*(\lambda)$ (the shock *existence* condition) or its shock *jump* condition. This is illustrated in figure 1, where equation (5) is plotted for two sets of n and p:
(1) $n = 1.75$, $p = 2$, used for the calculations presented in this paper,
(2) $n = 1.558$, $p = -0.162$, for which the MSD and full potential $\phi_x^*(\lambda)$ agree

very well for $0° < \lambda < 50°$. We have not yet computed wing surface pressures for this set of values. Other MSD equations of the same form but with different coefficients have recently been proposed, such as the NLR equation (ref. 5); $\phi_x^*(\lambda)$ for this equation is also plotted in figure 1.

MODIFICATIONS TO THE CLASSICAL SMALL-DISTURBANCE PROCEDURE AND DIFFERENCING TECHNIQUES FOR THE SUPERSONIC REGION

Use of an improved form of the governing equation does not, in itself, guarantee that shock waves will be properly captured by the computational method. The finite difference scheme used to solve the equation must: (1) enforce shock conditions consistent with the governing equation (this is guaranteed, in the limit of vanishing mesh spacing, by differencing the equation in conservation form), (2) be adaptable to a stable relaxation algorithm, and (3) avoid excessive dispersive or dissipative distortion of the shock profile.

In transonic flow relaxation methods, the mixed subsonic-supersonic character of the flow field is accounted for by the use of central differencing in subsonic regions and upwind differencing in supersonic regions. For the CSD equation the x-coordinate is the axis of the characteristic cone in supersonic regions. Thus, upwind differencing of the x derivatives and central differencing of the y and z derivatives leads to a numerical domain of dependence that always includes the mathematical domain of dependence; consequently, a necessary condition for stability is maintained. However, the characteristic cone axis for the MSD equation lies in a direction that corresponds to the local flow direction vector, which generally is not coincident with the x-direction. Differencing the MSD equation in supersonic regions in the same manner as the CSD equation can violate the domain of dependence restriction, thereby producing instabilities. We have investigated five supersonic difference schemes for modified equations in an attempt to find one with suitable stability and shock capturing properties. As in reference 3, only additional terms in the x and y directions are retained.

Scheme 1

In this scheme the CSD terms in the MSD equation are differenced in the same manner as for the CSD equation; the remaining terms are approximated by central differences. Thus, no account is taken of the local orientation of the stream direction vector. This procedure has the advantage that the equation can easily be differenced in conservation form. However, convergence properties of the relaxation process were found to be relatively poor. Furthermore, large overshoots at shock waves were observed in some cases.

Scheme 2

The principal part of equation (4) can be expressed in the canonical form

$$(a^2 - q^2)\phi_{ss} + a^2\phi_{nn} + a^2\phi_{zz} = 0 \tag{6}$$

where q and a are particle and sound speeds, and s and n are the local stream and stream-normal directions in the x-y plane. According to Jameson's (nonconservative) rotated differencing procedure (ref. 6), the ϕ_{xx}, ϕ_{xy}, ϕ_{yy} components of ϕ_{ss} and ϕ_{nn} should be upwind and central differenced, respectively, to maintain proper domains of dependence. An exact rotation of the MSD equation is unwieldy, so only an approximate rotation, such as the one in reference 5, is used for Scheme 2. Neglecting products of perturbation velocities gives for the terms in equation (6) (with n = p = 2)

$$(a^2 - q^2)/a_\infty^2 = 1 - M_\infty^2 - (\gamma + 1)M_\infty^2\phi_x \tag{7a}$$

$$\phi_{ss} = \phi_{xx} + 2\phi_y\phi_{xy} \tag{7b}$$

$$a^2/a_\infty^2 = 1 - (\gamma - 1)M_\infty^2\phi_x \tag{7c}$$

$$\phi_{nn} = -2\phi_y\phi_{xy} + \phi_{yy} \tag{7d}$$

Substituting equations (7) in equation (6) and again neglecting products of perturbation velocities gives the MSD equation in the split form

$$\underline{\left[1 - M_\infty^2 - (\gamma+1)M_\infty^2\phi_x\right]\phi_{xx} + 2(1 - M_\infty^2)\phi_y\phi_{xy}} - 2\phi_y\phi_{xy} + \left[1 - (\gamma - 1)M_\infty^2\phi_x\right]\phi_{yy} + \phi_{zz} = 0 \tag{8}$$

where the underlined terms are upwind differenced in supersonic regions, defined approximately by $\left[1 - M_\infty^2 - (\gamma + 1)M_\infty^2\phi_x\right] < 0$. The conservation form of equation (8) is

$$\underline{\left[(1 - M_\infty^2)\phi_x - \frac{(\gamma+1)}{2}M_\infty^2\phi_x^2 + (1 - M_\infty^2)\phi_y^2\right]_x} - \left\{\left[1 - \frac{(\gamma - 1)}{2}M_\infty^2\right]\phi_y^2\right\}_x + \left[\phi_y - (\gamma - 1)M_\infty^2\phi_x\phi_y\right]_y + \phi_{zz} = 0 \tag{9}$$

Equation (9) is equivalent to the splitting given in reference 5. The convergence properties of this scheme were found to be even worse than those of Scheme 1, and no computed results from either of these schemes are presented in this report.

Scheme 3

This scheme is also an approximate rotation of the MSD equation. In this case, however, the term $-2(\gamma + 1)M_\infty^2\phi_x\phi_y\phi_{xy}$ is not neglected, since $1 - M_\infty^2$ and $(\gamma + 1)M_\infty^2\phi_x$ can be of the same order. Thus, the approximation

$$\frac{(a^2 - q^2)}{a_\infty^2}\phi_{ss} = \left[1 - M_\infty^2 - (\gamma + 1)M_\infty^2\phi_x\right]\left[\phi_{xx} + 2\phi_y\phi_{xy}\right] \tag{10}$$

is used. Note that this term, in conjunction with

$$(a^2/a_\infty^2)\phi_{nn} \doteq -2\phi_y\phi_{xy} + (1 - (\gamma - 1)M_\infty^2\phi_x)\phi_{yy}$$

is not consistent with the MSD equation. However, this new splitting can be applied as follows. By defining the central difference approximation for the MSD equation (4) as $L(\phi) = 0$, one can write the rotated equation

$$L(\phi) + \bar{J}(\phi) - J(\phi) = 0 \tag{11}$$

where $\bar{J}$ and J are upwind and central difference approximations to equation (10), respectively. Unfortunately, equation (11) cannot be expressed in conservation form, and, for the computations presented in the next section, J from equation (10) was expressed in the form

$$J(\phi) = \left[(1 - M_\infty^2)\phi_x - \frac{(\gamma + 1)}{2}M_\infty^2\phi_x + (1 - M_\infty^2)\phi_y^2\right]_x - \underline{2(\gamma+1)M_\infty^2\phi_x\phi_y\phi_{xy}} \tag{12}$$

Hence, the complete equation is differenced conservatively except for the underlined term. The ϕ_{xy} part of this term in $\bar{J}(\phi)$ was upwind differenced in both x and y. The other term in equation (12) was upwind differenced only in x. Scheme 3 improved convergence and reduced shock overshoots relative to Scheme 1. Also, improved capture of weak swept shocks was observed, although overshoots occurred for stronger shocks in some cases.

Scheme 4

A less approximate and consistent (in the sense of Scheme 2) rotation can be accomplished by considering a second modified small-disturbance equation in the quasi-linear form

$$\left[1 - M_\infty^2 - (\gamma + 1)M_\infty^2\phi_x\right]\phi_{xx} - 2M_\infty^2\phi_y(1+\phi_x)\phi_{xy} + \left[1 - (\gamma - 1)M_\infty^2\phi_x\right]\phi_{yy} + \phi_{zz} = 0 \tag{13}$$

Note that the coefficient of ϕ_{xy} is precisely that of the full potential equation and cannot be put into conservation form. In this scheme the rotation angle is approximated by

$$\sin^2\theta = \frac{\phi_y^2}{1 + 2\phi_x}$$

$$\cos^2\theta = 1 \tag{14}$$

$$\sin\theta\cos\theta = \frac{(1 + \phi_x)\phi_y}{1 + 2\phi_x}$$

resulting in the approximations

$$\phi_{ss} = \phi_{xx} + \frac{2(1 + \phi_x)}{1 + 2\phi_x} \phi_y \phi_{xy}$$

and

$$\phi_{nn} = \frac{-2(1 + \phi_x)}{1 + 2\phi_x} \phi_x \phi_{xy} + \phi_{yy}$$

Thus, the split equation becomes

$$\left[1 - M_\infty{}^2 - (\gamma + 1) M_\infty{}^2 \phi_x\right]\left[\phi_{xx} + 2 \frac{(1 + \phi_x)}{(1 + 2\phi_x)} \phi_y \phi_{xy}\right]$$

$$+ \left[1 - (\gamma - 1) M_\infty{}^2 \phi_x\right]\left[\phi_{yy} - \frac{2(1 + \phi_x)}{(1 + 2\phi_x)} \phi_y \phi_{xy}\right] + \phi_{zz} = 0 \quad (15)$$

The less approximate trigonometric forms in equation (14) are necessary for equation (15) to be consistent with equation (13). Since the mathematics involved with equation (15) begins to approach that of the full potential equation in the x-y plane, this procedure was not tested but rather was abandoned in favor of Scheme 5.

Scheme 5

The MSD equation was modified to include all x-y derivitives in the full potential equation; the only z derivative retained was ϕ_{zz}. The equation was solved using Jameson's rotated differencing procedure, and Jameson's rules for constructing a stable relaxation algorithm were rigidly followed (see ref. 6 and appendices B and C of ref. 7). The relaxation process converged more rapidly than for the other schemes, and no shock overshoots were observed. However, the scheme is nonconservative and highly dissipative and tended to "smear" supersonic-to-supersonic shock waves.

The differencing in all schemes is complicated by the use of a transformation that maps the wing planform into a rectangle in the computational domain (refs. 1, 2, 4, 8). To "empirically correct" the (supersonic-to-subsonic) shock jumps for viscosity and thus improve the agreement in comparisons with experiment (refs. 3, 4, 8), the shock point operator was not used in any of the computations in this report.

CSD AND MSD COMPUTATIONS FOR THE ROCKWELL HiMAT RPRV

An example that demonstrates the usefulness of small-disturbance theory and illustrates the effect of the extra terms in the MSD equation is provided by computations for the HiMAT RPRV (highly maneuverable aircraft technology, remotely piloted research vehicle). A three view of the original HiMAT

configuration is shown in figure 2. At the maneuver design point for this configuration, the drag exceeded the design goal by several hundred counts. It was decided that the design goal could not be achieved, within the specified budget and calendar time constraints, by modifying the configuration using the traditional experimental "cut and file" approach. Rockwell therefore adopted and developed the following integrated design procedure: (1) establish base-line comparisons of experimental and computed surface pressures obtained using the Bailey-Ballhaus Transonic Wing Code (CSD), (2) "cut and file" computationally (rather than experimentally), and (3) verify experimentally.

A sample base-line comparison of CSD and experimental results is shown in figure 3. (The canard was omitted in both the experiment and the calculations.) The agreement at mid-semi-span is satisfactory. However, in the outboard region, where the flow is nearly two-dimensional in a plane normal to the sweep direction, the CSD code performed poorly. Consequently, the inboard 70 percent of the semi-span, where the flow was highly three-dimensional, was redesigned using the Bailey-Ballhaus code. The outboard 30 percent was analyzed and modified using the Garabedian-Korn two-dimensional program and sweep theory. The redesign weakened and swept embedded shock waves, reducing the extent of flow separation and reducing the drag to within a few counts of the design goal.

The HiMAT example pointed out the need for the extra terms in the governing equation for swept wing configurations. These terms were subsequently added; computed results using Schemes 3 and 5 are compared with the CSD and experimental results in figure 3. Results computed using Scheme 1 were very similar to those of Scheme 3 except the shock overshoot was greater. The more dissipative Scheme 5 shows no such overshoot.

THE DOUBLE SHOCK CONFIGURATION ON THE ONERA M-6 WING

Figure 4 shows a planform view of the ONERA M-6 wing along with the double shock configuration that occurs for $M_\infty = 0.84$, $\alpha = 3°$. Within the supersonic region there is a swept (35°), supersonic-to-supersonic shock wave, sometimes referred to as a "conical shock." Further downstream there is a less highly swept shock wave that terminates the supersonic region. The two shocks intersect to form a strong, unswept shock near the tip.

Computed CSD and experimental wing surface pressures for this condition were compared in reference 8. Satisfactory agreement was obtained except for the failure of the computations to resolve the relatively weak conical shock. It was mentioned that the use of the MSD equation should correct this deficiency. CSD and MSD solutions have been computed on a grid with points clustered in the vicinity of the conical shock. The results, compared with ONERA experimental data, are shown in figure 5. Section pressures for the MSD equation (Scheme 3) indicate the existence of a conical shock; those for the CSD equation do not. MSD results are also compared (fig. 6) with fine grid computations run by Mr. Ray Hicks of NASA Ames Research Center using the new full potential wing code written by Jameson (ref. 6). The Jameson code is based on the nonconservative rotated difference scheme; the conical shock is badly smeared at $\eta = 0.75$ and is totally smeared at $\eta = 0.8$. Scheme 5, which also uses the full potential

formulation with the nonconservative rotated difference scheme (for the x and y derivatives), produced the same smearing of the conical shock. Scheme 1 properly captured the conical shock but produced a large overshoot at the head of the downstream shock.

CONCLUDING REMARKS

Comparisons of computed and experimental surface pressures for the HiMAT wing (fig. 3b) and the ONERA M-6 wing (fig. 5) illustrate the importance of retaining additional terms in the governing equations, as suggested in reference 3. Inclusion of these terms permitted the capture of shock waves for both configurations that had been observed experimentally, but were not resolved by the CSD theory. Five schemes for differencing the small disturbance equation, modified with additional terms, have been discussed. It was determined from numerical tests that Scheme 3 performed best in treating cases with multiple embedded shock waves. Scheme 5 demonstrated the best convergence properties and produced results nearly indistinguishable (except at the leading edge) from those obtained from Jameson's code (ref. 6). However, because of its nonconservative and dissipative properties, this scheme gives relatively poor resolution of the conical shock wave on the ONERA M-6 wing.

REFERENCES

1. Ballhaus, W. F.; and Bailey, F. R.: Numerical Calculation of Transonic Flow About Swept Wings. AIAA Paper 72-677, June 1972.

2. Bailey, F. R.; and Ballhaus, W. F.: Relaxation Methods for Transonic Flow About Wing-Cylinder Combinations and Lifting Swept Wings. Lecture Notes in Physics, vol. 19, Springer-Verlag, 1972, pp. 2-9.

3. Lomax, H.; Bailey, F. R.; and Ballhaus, W. F.: On the Numerical Simulation of Three-Dimensional Transonic Flow with Application to the C-141 Wing. NASA TN D-6933, 1973.

4. Ballhaus, W. F.: Some Recent Progress in Transonic Flow Computations. VKI Lecture Series, "Computational Fluid Dynamics," Von Karman Institute for Fluid Dynamics, Rhode-St.-Genese, Belgium, March 15-19, 1976.

5. Van der Vooren, J.; Sloof, J. W.; Huizing, G. H.; and van Essen, A.: Remarks on the Suitability of Various Transonic Small-Perturbation Equations to Describe Three-Dimensional Flow; Examples of Computations Using a Fully-Conservative Rotated Difference Scheme. Presented at the Symposium Transsonicum II, September 1975.

6. Jameson, A.: Transonic Flow Calculations, VKI Lecture Series, "Computational Fluid Dynamics," Von Karman Institute for Fluid Dynamics, Rhode-St.-Genese, Belgium, March 15-19, 1976.

7. South, J. C.; and Keller, J. D.: Axisymmetric Transonic Flow Including Wind Tunnel Wall Effects. NASA SP-347, 1975, pp. 1233-1267.

8. Bailey, F. R.; and Ballhaus, W. F.: Comparisons of Computed and Experimental Pressures for Transonic Flows About Isolated Wings and Wing-Fuselage Configurations. NASA SP-347, 1975, pp. 1213-1231.

9. Monnerie, B.; and Charpin, F.: Essais de Buffeting d'une Aile en Fleche en Transsonique. 10e Colloque D'Aérodynamique Appliquée, November, 1973.

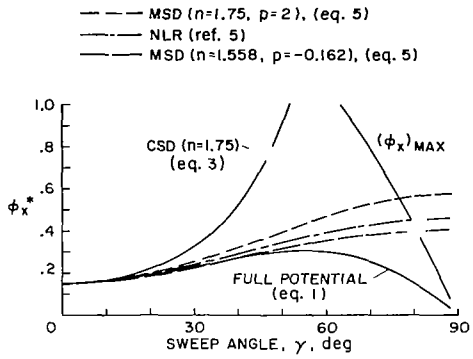

Figure 1.- Shock existence condition $\left[\phi_x^* < \phi_x < (\phi_x)_{MAX}\right]$ as a function of sweep angle.

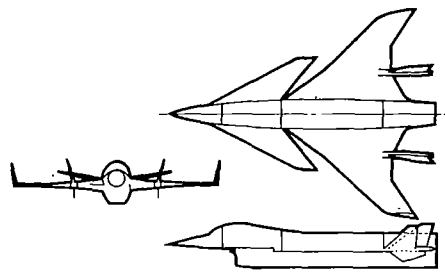

Figure 2.- HiMAT RPRV three-view.

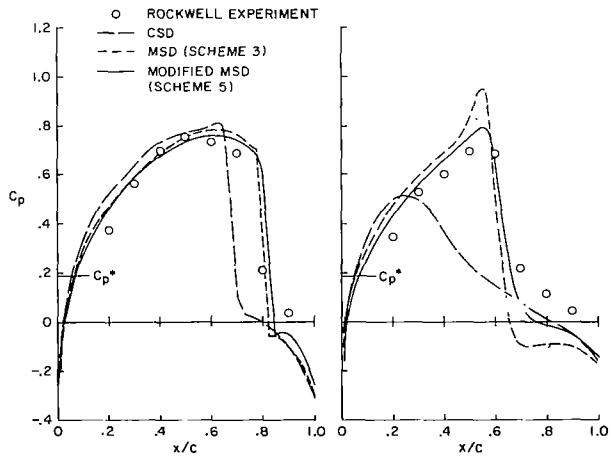

Figure 3.- Surface pressure coefficients on the HiMAT RPRV, $M_\infty = 0.9$, $\alpha = 5°$.

(a) 55 percent semi-span station.

(b) 85 percent semi-span station.

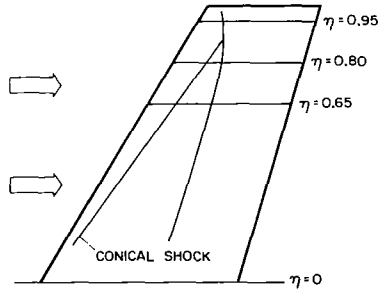

Figure 4.- Planform view of the ONERA M-6 wing showing double shock configuration for $M_\infty = 0.84$, $\alpha = 3°$.

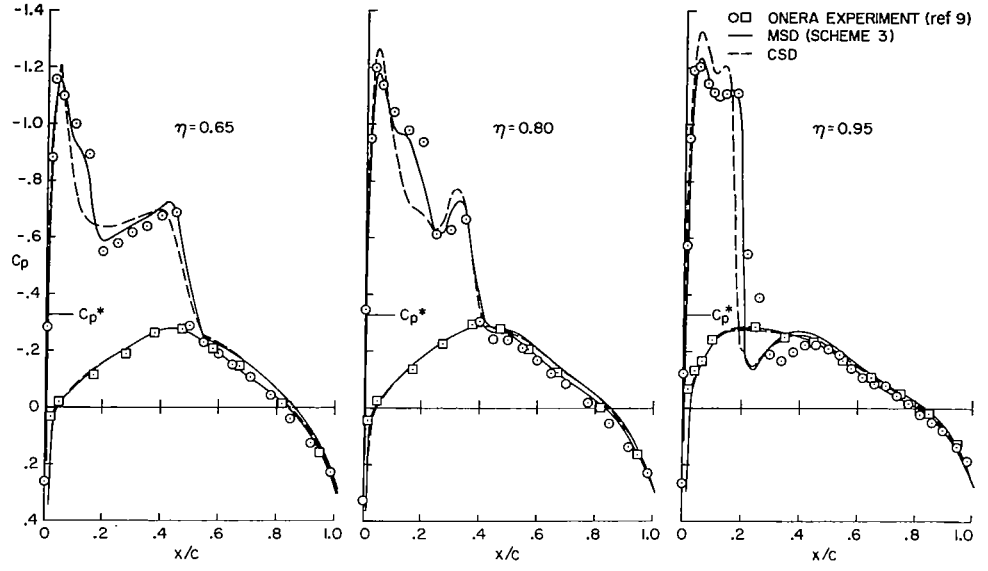

Figure 5.- Computed and experimental surface pressures for the ONERA M-6 wing, $M_\infty = 0.84$, $\alpha = 3°$.

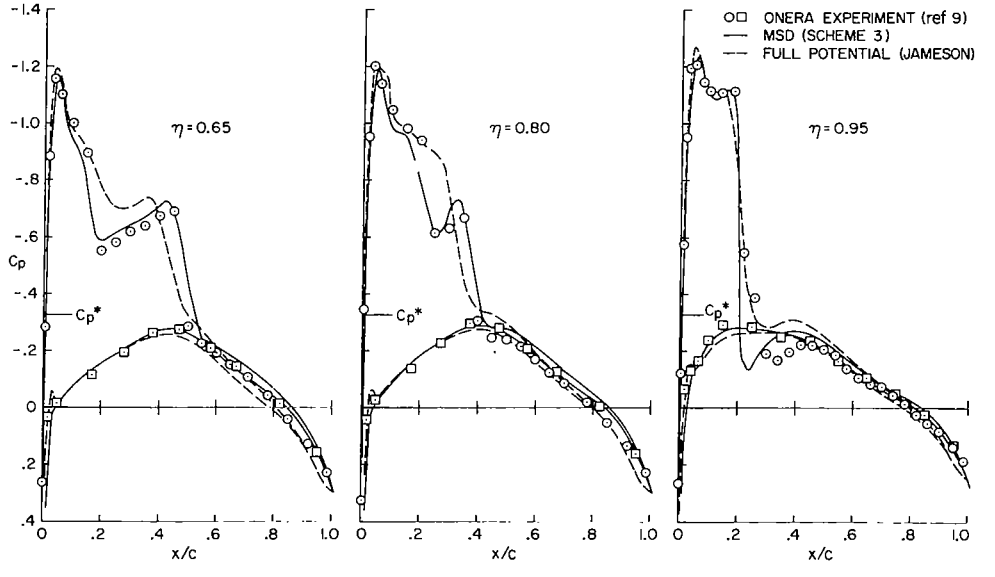

Figure 6.- Computed and experimental surface pressures for the ONERA M-6 wing, $M_\infty = 0.84$, $\alpha = 3°$.